Excited States of Phosphorescent Platinum(II) Complexes Containing N∧C∧N-Coordinating Tridentate Ligands: Spectroscopic Investigations and Time-Dependent Density Functional Theory Calculations

Wataru Sotoyama,*,† Tasuku Satoh,† Hiroyuki Sato, Azuma Matsuura, and Norio Sawatari

Fujitsu Laboratories Ltd., 10-1 Morinosato−Wakamiya, Atsugi 243-0197, Japan

Received: June 22, 2005; In Final Form: September 4, 2005

The absorption and emission spectra of the Pt(II) complexes containing N∧C∧N-coordinating tridentate ligands, platinum(II) 1,3-di(2-pyridyl)benzene chloride [Pt(dpb)Cl] and platinum(II) 3,5-di(2-pyridyl)toluene chloride [Pt(dpt)Cl], together with their corresponding free ligands, 1,3-di(2-pyridyl)benzene (dpbH) and 3,5-di(2-pyridyl)toluene (dptH), have been analyzed by density functional theory (DFT) for the ground state and time-dependent DFT (TDDFT) for the excited states. $T_1(A_1)$ and $S_1(B_2)$ of the complexes (in C_{2v} symmetry) were assigned on the basis of the calculated excitation energies as well as comparison of the experimental spectroscopic properties and the calculated states' characteristics. The calculated excitation energies for T_1 and S_1 of the complexes as well as those for T_1 of the free ligands were in good agreement with their observed values within 600 cm^{-1}. The d−π* characters of the excited states were evaluated from the change in electron densities between the ground and excited states by Mulliken population analysis; values of 25% for T_1 and 32% for S_1 were obtained for both complexes. The calculated values of d−π* character were found to be consistent with the reported emission lifetimes as well as the observed emission energy shifts from the corresponding free ligands. Most spectroscopic properties of the complexes and the free ligands, which include solvatochromic shift, Stokes shifts, methyl substitution shifts, and emission spectra profiles, were well explained from the calculation results.

1. Introduction

Studies on phosphorescent transition-metal complexes are of particular interest not only from a scientific viewpoint but also in development of emissive dopants for phosphorescent organic light-emitting diodes (OLEDs).[1,2] The rapid growth of interest in phosphorescent OLEDs has prompted syntheses and photophysical investigations of a wide variety of phosphorescent complexes.[3−7] Recently, a new class of platinum(II) complexes consisting of platinum, chloride, and N∧C∧N-coordinating tridentate ligands [platinum(II) 1,3-di(2-pyridyl)benzene chloride, Pt(dpb)Cl, and platinum(II) 3,5-di(2-pyridyl)toluene chloride, Pt(dpt)Cl, Figure 1] have been synthesized,[8,9] and high phosphorescence quantum yields ranging from 0.58 to 0.68 in solution at room temperature have been reported in these complexes.[9] Pt(dpt)Cl and its derivative with a phenoxide group that replaces the chloride have been reported to exhibit remarkable performance as emissive dopants of OLEDs.[10]

The lowest excited triplet states (T_1) of Pt(dpb)Cl and Pt(dpt)Cl have been assigned to primarily ligand-centered (LC) $^3\pi-\pi^*$ character from their highly structured emission profile with very small Stokes shifts and relatively long emission lifetimes [Pt(dpb)Cl 7.2 μs and Pt(dpt)Cl 7.8 μs in solution at room temperature].[9] However, these emission lifetimes are not much longer than those of the complexes, which have the triplet-emitting states with metal-to-ligand charge transfer (MLCT) character. For example, in the case of $Ir(ppy)_3$, where ppy represents 2-phenylpyridine ligand, the emitting states have been assigned to be mainly ^{3}MLCT character by theoretical studies[11] and spectroscopic measurements.[12] The emission lifetimes of this complex were found to be 2 μs and 5 μs at room temperature and 77 K, respectively, in solution.[13] Taking into account the possible admixture of $\pi-\pi^*$/d−π* (MLCT) character, which is common for T_1 of many phosphorescent transition-metal complexes,[14−20] it is expected that the d−π* character would participate in T_1 of Pt(dpb)Cl and Pt(dpt)Cl. The d−π* admixture to an excited state, especially to T_1, is important even though the state character is primary $\pi-\pi^*$, since a small amount of d−π* character can dominate the kinetics of the deactivation processes of the excited state by its strong spin−orbit coupling ability to the states with different spin multiplicities.[16,17,21−23]

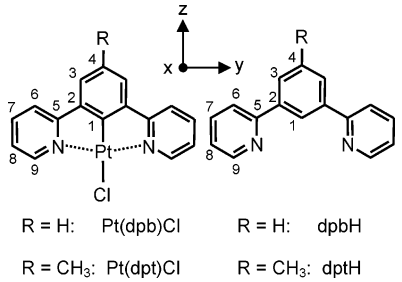

Figure 1. Schematic structure of the two complexes [Pt(dpb)Cl and Pt(dpt)Cl] and the two free ligands [dpbH and dptH] along with the molecular axis. The numbers in the structures designate each carbon atom.

In this paper we describe detailed analysis of the excited states of Pt(dpb)Cl and Pt(dpt)Cl by correlating the spectroscopic data with the calculation results based on density functional theory (DFT). The main objectives of this study are assignment of the

* To whom correspondence should be addressed: e-mail wataru_sotoyama@fujifilm.co.jp.

† Present address: Advanced Core Technology Laboratories, Fuji Photo Film Co., Ltd., 210 Nakanuma, Minamiashigara 250-0193, Japan.

10.1021/jp053366c CCC: $30.25
Published on Web 10/11/2005

TABLE 1: Calculated and Observed X-ray Crystallographic Data for Representative Bond Lengths (Å) and Angles (degree) for Pt(dpb)Cl[a]

bond[b]	calcd	obsd[c]
Pt−Cl	2.471	2.417
Pt−C(1)	1.926	1.907
Pt−N	2.065	2.037[d]
C(1)−Pt−N	80.43	80.5[d]
Pt−C(1)−C(2)	118.62	119.2[d]
Pt−N−C(5)	113.95	114.6[d]

[a] Bond lengths are given in angstroms; bond angles are given in degrees. [b] See Figure 1 for numbering of the carbon atoms. [c] Data from ref 8. [d] Average of two equivalent data points.

low-lying excited states of the complexes and quantitative evaluation of the d−π* character at the complexes. The free tridentate ligands [1,3-di(2-pyridyl)benzene (dpbH) and 3,5-di-(2-pyridyl)toluene (dptH), Figure 1] are also investigated to assist in analysis of the excited states of the complexes. Several aspects of the spectroscopic features, such as effect of methyl substitution on the excitation energies and the difference in emission profile between the complexes and the free ligands, will be discussed in light of the calculation results by DFT and time-dependent DFT (TDDFT).

2. Experimental Section

2.1. Materials and Spectroscopic Measurements. Pt(dpb)-Cl and Pt(dpt)Cl were synthesized from dpbH and dptH, respectively, according to the literature.[8,9] Absorption and emission measurements in solution were conducted in 1 cm path length quartz cuvettes at room temperature or in 5 mm diameter quartz tubes at 77 K. Absorption spectra were recorded on a Hitachi U-4100 spectrophotometer. Emission spectra of Pt(dpb)-Cl and Pt(dpt)Cl were measured on a Minolta CS-1000 spectroradiometer, equipped with an ultra-high-pressure mercury lamp and a visible blocking filter, as the excitation source. The solutions of free ligands (dpbH and dptH) showed phosphorescence with lifetimes of a few seconds at 77 K; phosphorescence spectra of these solutions were measured with a phosphoroscope in addition to the above apparatus.

2.2. Computational Details. The ground-state DFT and the excited-state time-dependent DFT (TDDFT)[24−26] calculations were carried out with the Gaussian98 program package.[27] TDDFT has been successfully applied to excited-state calculations for many transition-metal complexes.[11,28−34] All calculations were carried out with the LANL2DZ basis set with the relativistic effective core potential (ECP) for Pt[35] and the 6-31G* basis set for the other elements. The calculation results (orbitals and densities) were plotted with the visualization program (xmo 4.0) in MOPAC2002.[36] Calculations on the electronic ground state (S_0) of the complexes [Pt(dpb)Cl and Pt(dpt)Cl] and the free ligands (dpbH and dptH) were carried out by use of B3LYP density functional theory.[37,38] The S_0 geometries were optimized under symmetry constraints of C_{2v} for Pt(dpb)Cl and C_s (*zx* symmetry plane, Figure 1) for Pt(dpt)Cl. The optimized planar geometries of these complexes were confirmed by the vibrational frequencies calculations with no imaginary frequencies. The optimized geometry of Pt(dpb)Cl was found to be in good agreement with the X-ray crystallographic data (Table 1).[8] For dpbH and dptH, the geometries optimized within symmetry constraints similar to the complexes (planar forms) were different from those fully optimized without symmetry constraints (twisted forms). Although the twisted forms have lower S_0 total energy than the planar forms for both dpbH and dptH, the differences in the S_0 total energy between the planar and twisted forms were found to be negligible (158 cm^{-1} for dpbH and 179 cm^{-1} for dpbH). On the basis of the minor energy deviations from the twisted forms, we present calculation results at the planar forms of the free ligands in this study for convenience of comparison with the results for the complexes. The geometries for the lowest excited triplet states (T_1) of Pt(dpb)Cl and dpbH were optimized at the restricted open-shell B3LYP level.

At the respective optimized geometries, TDDFT calculations with the B3LYP functional were carried out. Ten lowest roots for triplet states as well as singlet states were calculated for the complexes and the ligands. In addition to the vertical excitation energies for all calculated roots, the one-particle densities and the dipole moments for the three lowest triplet and singlet roots were obtained for the complexes.

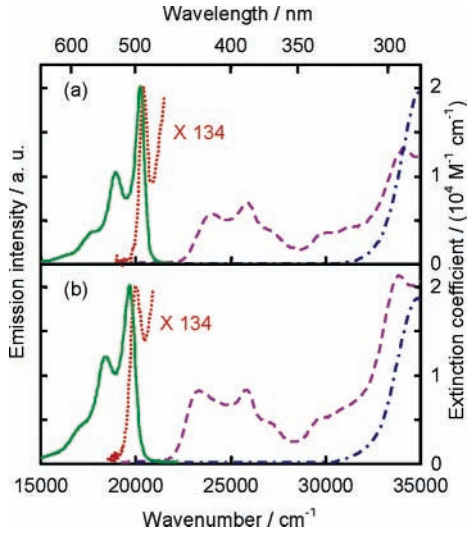

Figure 2. Absorption and emission spectra of the complexes along with absorption spectra of the free ligands in toluene at room temperature: (a) Pt(dpb)Cl and dpbH; (b) Pt(dpt)Cl and dptH. Solid line (green), emission of the complexes; dashed line (purple), absorption of the complexes; dotted line (red), absorption of the complexes in an expanded scale (134 times); dashed−dotted line (blue), absorption of the free ligands.

3. Results

3.1. Absorption and Emission Spectra at Room Temperature. Figure 2 shows absorption and emission spectra of Pt-(dpb)Cl (a) and Pt(dpt)Cl (b) together with the absorption spectra of dpbH (a) and dptH (b) in toluene at room temperature. The spectra of the complexes in Figure 2 replicate the results reported by Williams et al.[9] The lowest energy weak peaks in Pt(dpb)Cl and Pt(dpt)Cl absorption spectra are assigned as S_0-T_1 absorption by their mirror-symmetry relation with the emission peak. The strong absorption envelopes at 22 000−30 000 cm^{-1} are assigned to the absorptions to the singlet excited states with significant MLCT character involving Pt and Cl orbitals from the comparison with the absorption spectra of the free ligands. The lowest energy peak among these absorptions is considered as the S_1 peak of the each complex. (Strictly speaking, the absorption spectra do not exclude the possibility of the existence of one or more singlet excited states with very small absorption cross sections at the lower energy side of the S_1 peak assigned above. However, even if there are such dark states, the discussion about the orbital assignment of the S_1 peak based on the absorption intensities in section 4.1 still remains unchanged.)

TABLE 2: T_1 and S_1 Absorption Peak Energies for Pt(dpb)Cl and Pt(dpt)Cl in Toluene and Acetonitrile at Room Temperature

		absorption peak energy/cm^{-1}	
complex	state	toluene	acetonitrile
Pt(dpb)Cl	T_1	20 400	20 700
Pt(dpb)Cl	S_1	24 000	25 200
Pt(dpt)Cl	T_1	20 000	20 300
Pt(dpt)Cl	S_1	23 400	24 500

We observed negative solvatochromic behavior (peak blue shift with increasing solvent polarity) reported in ref 9 for S_1 and T_1 peaks of Pt(dpb)Cl and Pt(dpt)Cl in several solvents. The absorption peak energies in toluene and acetonitrile are presented in Table 2. (See ref 9 for further information about spectral data in various solvents including toluene and acetonitrile.) According to the theoretical study on solvent effect by Marcus,[39,40] negative solvatochromic behavior of an absorption peak has been interpreted to be associated with the decrease in dipole moments by excitation. It is observed that the solvatochromic shifts are fairly larger for S_1 peaks than T_1 peaks, which would suggest a lager decrease in dipole moment by the S_0-S_1 excitation than that of the S_0-T_1 excitations of these complexes.

3.2. Phosphorescence Spectra at 77 K. Figure 3 shows the phosphorescence spectra of dpbH and Pt(dpb)Cl (a) and of dptH and Pt(dpt)Cl (b) in toluene at 77 K. The highest energy peak of each spectrum (presented in Tables 3 and 4) is attributed to the vibrational 0−0 origin of the T_1-S_0 transition. The phosphorescence origins of the Pt(dpb)Cl and Pt(dpt)Cl have red-shifted 2200 and 2580 cm^{-1} from those of the corresponding free ligands, respectively. These shifts are much larger than those for complexes with ligand-centered emitting states in the literature, such as $[Pt(bpy)_2]^{2+}$ (950 cm^{-1}) or $[Rh(bpy)_3]^{3+}$ (600 cm^{-1}),[41] where bpy is 2,2′-bipyridine, suggesting significant admixture of the metal character in the emitting state of the complexes. The relative intensity of the origin peak, compared to the peaks of vibrational satellites with frequencies of about 1300 cm^{-1}, would become notably larger for the complexes than for the free ligands; these features imply closer equilibrium geometries between S_0 and T_1 for these complexes compared to those for the free ligands. Similar trends have been observed for complexes having T_1 with significant MLCT character, such as $[Ru(bpy)_3]^{2+}$or $Pt(thpy)_2$, where thpy is 2-(2-thienyl)pyridine, in comparison with their corresponding free ligands.[17,18,42] The characteristics such as the position and profile of the spectra

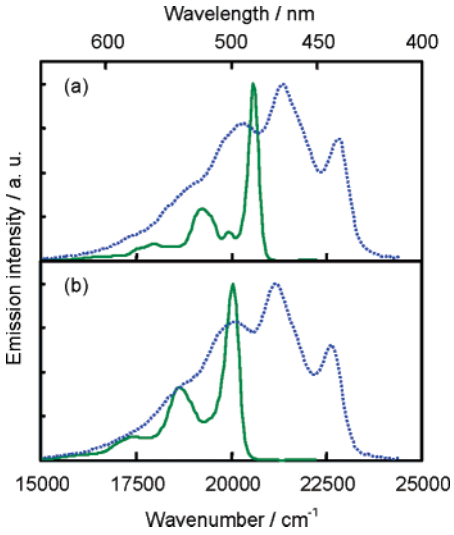

Figure 3. Emission spectra of the complexes and the free ligands in toluene at 77 K: (a) Pt(dpb)Cl and dpbH; (b) Pt(dpt)Cl and dptH. Solid line (green), emission of the complexes; dotted line (blue), emission of the free ligands measured with a phosphoroscope.

indicate a certain amount of metal d-orbital admixture to T_1 of Pt(dpb)Cl and Pt(dpt)Cl.

The methyl substitution in place of the hydrogen atom at C(4) of the phenyl ring causes somewhat different effects to the emission spectra between the complexes and the free ligands. Both the methyl-substituted complex [Pt(dpt)Cl] and free ligand (dptH) displayed red-shifted emission from their unsubstituted counterparts [Pt(dpb)Cl and dpbH]. However, the spectral shift was found to be substantially greater between the complexes (540 cm^{-1}) than between the free ligands (160 cm^{-1}). This large difference in methyl-substitution effect would suggest the orbital nature difference of T_1 between the complexes and the free ligands.

4. Theoretical and Experimental Data Comparison

4.1. Assignments and Excitation Energies of Calculated Roots. Figure 4 depicts the four highest occupied and the two lowest unoccupied molecular orbitals (HOMOs and LUMOs) of Pt(dpb)Cl, as well as the HOMO and LUMO of dpbH obtained from the ground-state DFT calculations. The HOMOs and LUMOs for Pt(dpt)Cl and dptH are similar in shape with the corresponding orbitals presented in Figure 4. Every four

TABLE 3: Parameters[a] from Ground-State DFT and TDDFT Calculations for the Three Lowest Excited Triplet and Singlet Roots of Pt(dpb)Cl and Pt(dpt)Cl at the Ground-State Geometries

root			Pt(dpb)Cl			Pt(dpt)Cl		
(assignment[b])	symmetry[c]	dominant excitation[c,d]	E/cm^{-1}	μ_z ($\Delta\mu_z$)/D	f	E/cm^{-1}	μ_z ($\Delta\mu_z$)/D	f
ground state								
S_0	$^1A_1$			6.64			7.07	
triplet root								
1 (T_1)	$^3A_1$	$b_1 \rightarrow b_1^*$	20 421	5.51 (−1.13)		20 059	6.69 (−0.38)	
2 (T_2)	$^3B_2$	$b_1 \rightarrow a_2^*$	20 892	1.03 (−5.61)		20 270	2.66 (−4.41)	
3 (T_3)	$^3A_1$	$a_2 \rightarrow a_2^*$	22 993	4.41 (−2.23)		22 886	5.09 (−1.98)	
T_1 (expt[e])			20 580			20 040		
singlet root								
1 (S_1)	$^1B_2$	$b_1 \rightarrow a_2^*$	23 489	−2.43 (−9.07)	0.074	23 120	−1.04 (−8.10)	0.077
2 (S_2)	$^1A_1$	$b_1 \rightarrow b_1^*$	23 707	3.06 (−3.58)	0.007	23 342	4.64 (−2.43)	0.006
3 (S_3)	$^1A_2$	$b_2 \rightarrow b_1^*$	25 928	−4.95 (−11.58)	0.000	25 899	−4.47 (−11.54)	0.000
S_1 (expt[f])			24 000			23 400		

[a] E, vertical excitation energy; μ_z, z component of dipole moment; $\Delta\mu_z$, dipole moment differences between ground and excited states; f, oscillator strength. Experimental excitation energies are also listed. [b] See text. [c] Symmetry of states and orbitals are designated for Pt(dpb)Cl (C_{2v}, see Figure 1). [d] For designation of the orbitals, see Figure 4. [e] Phosphorescence 0−0 peak energy in toluene at 77 K. [f] Absorption peak energy in toluene at room temperature.

TABLE 4: Vertical Excitation Energies (*E*) from TDDFT Calculations for Triplet Excited States of DpbH and DptH with Experimental Excitation Energies

root (assignment[a])	symmetry[b]	dominant excitation[b],[c]	E/cm^{-1} dpbH	E/cm^{-1} dptH
1 (T_1)	$^3A_1$	$a_2 \rightarrow a_2^*$	23 344	23 217
2 (T_2)	$^3B_2$	$b_1 \rightarrow a_2^*$	27 304	27 077
T_1 (expt[d])			22 780	22 620

[a] See text. [b] Symmetry of states and orbitals are designated for dpbH (C_{2v}, see Figure 1). [c] For designation of the orbitals, see Figure 4. [d] Phosphorescence 0−0 peak energy in toluene at 77 K.

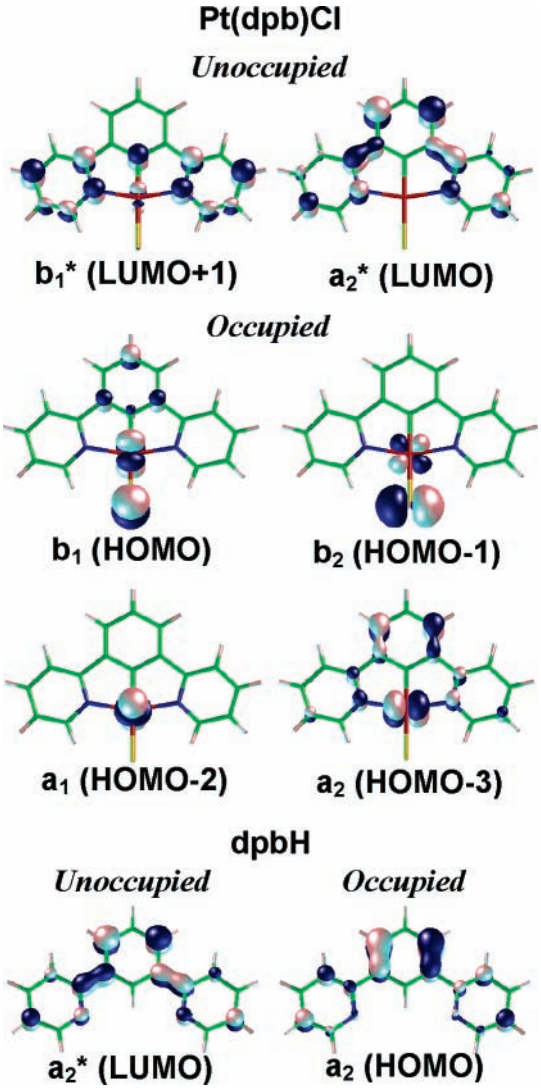

Figure 4. Contour plots of the two lowest unoccupied and the four highest occupied molecular orbitals of Pt(dpb)Cl, along with the LUMO and HOMO of dpbH.

HOMOs of the complexes are characterized by significant admixtures by the Pt d-orbitals. Two of them [b_1(HOMO) and a_2(HOMO-3)] are represented by combinations of d orbitals of the Pt and π orbitals of the tridentate ligand and Cl, while the remainder [b_2(HOMO-1) and a_1(HOMO-2)] have σ characters that are symmetrical about the molecular plane. On the other hand, the LUMOs correspond to the π^* orbitals almost localized in the ligand.

Table 3 summarizes the TDDFT calculation results of the properties that include dominant orbital excitations, vertical excitation energies (E), dipole moments (z component, μ_z), dipole moment differences from S_0 ($\Delta\mu_z$), and oscillator strengths (f) of the lowest three triplet and the lowest three singlet roots for Pt(dpb)Cl and Pt(dpt)Cl. Table 3 also includes the observed excitation energies for T_1 (the origins in the low-temperature phosphorescence spectra) and S_1 (the absorption peaks in the room-temperature spectra). The lowest three triplet roots as well as the lowest two singlet roots are represented by dominant excitations from mixed dπ orbitals to π^* orbitals. The third lowest singlet root is represented by a d$\sigma-\pi^*$ excitation. Excitations with d$\sigma-\pi^*$ character appear at the fifth lowest and higher roots for triplet states that are not specified in Table 3. The lowest three triplet as well as singlet roots for Pt(dpt)Cl are identical in characteristics of dominant excitations to the counterparts of Pt(dpb)Cl. In succeeding sections, we discuss only about Pt(dpb)Cl and dpbH, unless the methyl substitution effect is explored.

We begin the discussion on the comparison of the calculated and experimental data by assignment of T_1 and S_1 from the calculated triplet and singlet roots for Pt(dpb)Cl. Experimental evidence is needed for the T_1 and S_1 assignments because both the calculated energy differences between the two lowest roots of triplet as well as singlet are very small. On the other hand, the third lowest roots for triplet and singlet are excluded from the T_1 or S_1 assignment because they are calculated to be energetically well above the lowest two roots. Considering that the excitation to S_1 has a substantial extinction coefficient in the absorption spectrum (section 3.1), the lowest calculated singlet root ($^1B_2$; $f = 0.074$) is assigned to be S_1 since the second lowest root ($^1A_1$; $f = 0.007$) is predicted to have 1 order smaller absorption intensity. The calculated S_1 has a large $\Delta\mu_z$ (−9.07 D) that is consistent with the experimentally obtained large negative solvatochromic shift of the S_1 peak.[39,40] On the other hand, T_1 of Pt(dpb)Cl has different spectral characteristics from S_1 as discussed in section 3.1. Therefore, we assign the lowest calculated triplet root ($^3A_1$) to T_1 on the basis of the different dominant orbital excitation from S_1 ($^1B_2$) and the small $\Delta\mu_z$ (−1.13 D) that explain the small negative solvatochromic shift along with the small Stokes shift of the T_1 peak.[39] The second and third lowest calculated triplet (or singlet) roots are assigned to be T_2 and T_3 (or S_2 and S_3), respectively.

The calculated T_1 excitation energies of Pt(dpb)Cl and Pt(dpt)Cl show excellent agreements with the respective experimental phosphorescence origins at 77 K; the differences between the calculated and experimental values are found to be less than 200 cm^{-1}. In these comparisons, the calculated energies represent the vertical excitation energies at S_0 geometries, while the experimental energies correspond to the 0−0 transitions. However, these comparisons may be justified by the phosphorescence spectra, which indicate close equilibrium geometries between S_0 and T_1 of these complexes, as shown in section 3.2. (Geometries of T_1 together with the adiabatic excitation energies will be discussed in section 4.3.) The calculated S_1 excitation energies of the complexes also show good conformity with the experimental absorption peak energies within 600 cm^{-1}. Although TDDFT is known to have irregularities in description of long-range charge-transfer excited states,[43−45] the above calculation results for excitation energies ensure the applicability of the TDDFT calculations for T_1 and S_1 of the concerned molecules. Hence we further investigate the characteristics of T_1 and S_1 of the complexes by use of the TDDFT calculation results in the following sections.

TDDFT calculations were also carried out for the free ligands. Calculated vertical excitation energies and excitation types for the two lowest excited triplet roots of dpbH and dptH are summarized in Table 4 together with the experimental energies

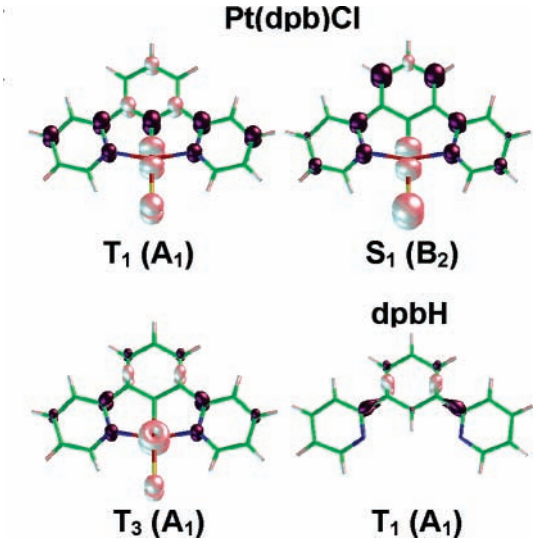

Figure 5. Contour plots of changes in electron densities for T_1, S_1, and T_3 from S_0 of Pt(dpb)Cl, along with that for T_1 from S_0 of dpbH.

of the phosphorescence origin. For dpbH, the lowest calculated triplet root ($^3A_1$) was assigned to be T_1 on the basis of the large energy separation between the first and second lowest roots. The small differences between the calculated and experimental T_1 excitation energies of dpbH and dptH (560−600 cm^{-1}) evidenced the accuracy of the TDDFT calculations.

4.2. Evaluation of d−π* Character in the Excited States. Evaluation of the degree of d−π* participation for low-lying excited states of mixed π−π*/d−π* character would be very helpful to understand the photophysical properties of the phosphorescent complexes. The zero-field splittings (ZFS) of sublevels of T_1 are shown to be a valuable experimental parameter to measure the metal participation in T_1 of complexes.[17−19] Theoretical calculation is considered to be an alternative for the evaluation of the metal participation that can be applied to a variety of complexes. The theoretical studies reported so far treat the evaluation of d−π* participation by several methods: the population analysis of orbitals involved in dominant excitations,[11] the analysis of distribution of spin densities and atomic charges by SCF calculations in T_1,[30] and the population analysis of metal atoms[46] or the metal d-orbitals for the ground and excited states.[47] We employed the population analysis of metal orbitals in combination with TDDFT calculations as discussed in the following section.

We have noted that T_1 and S_1 of the concerned complexes are each represented by a dominant excitation from a mixed dπ orbital to a π* orbital. More detailed pictures of the excited states depicting the changes in electron density[48] are provided in Figure 5, for T_1, S_1, and T_3 from S_0 of Pt(dpb)Cl along with that for T_1 from S_0 of dpbH. (The changes for T_2 and S_2 of the complex bear resemblances to those for S_1 and T_1, respectively.) T_1 and S_1 of Pt(dpb)Cl are characterized by d-electron density decrease on Pt and π-electron densities on Cl and some of the carbons in the tridentate ligand and by increases of π-electron densities of the tridentate ligand with respect to S_0, which indicate an admixture of d−π* and π−π* characters in each excited states.

Considering that TDDFT is a single excitation theory,[49] the decrease in d-electron densities calculated by TDDFT approximately gives the percentage of d−π* character in the excited state; that is, one electron decrease in d-electron densities represents 100% d−π* character. The decreases in d-electron densities for T_1 and S_1 of Pt(dpb)Cl are evaluated by Mulliken population analysis.[46,47] Table 5 summarizes the orbital populations of the Pt consisting of atomic orbitals s, p_π, p_σ, d_π, and d_σ (π and σ denote antisymmetric and symmetric orbitals about the molecular plane, respectively) for S_0, T_1, and S_1 of Pt(dpb)Cl and Pt(dpt)Cl. The differences between the two complexes are insignificant, and the s, p_σ, and d_σ densities remain unchanged by the T_1 and S_1 excitations. The d_π densities decrease in T_1 by 0.25e and in S_1 by 0.32e from S_0 for both of the complexes, suggesting the percentages of d−π* character in T_1 and S_1 as 25% and 32%, respectively. On the other hand, the p_π densities on Pt increase in T_1 by 0.06e [Pt(dpb)Cl] and 0.05e [Pt(dpt)Cl] from S_0, which indicates some delocalization of the spreading of the π* orbitals over the Pt atom.

The emitting states (T_1) of Pt(dpb)Cl and Pt(dpt)Cl with 25% d−π* character seem to fall into the intermediate category of significant LC/MLCT admixture in the sequence of complexes ordered by metal−d character (from pure LC to pure MLCT) of the emitting states.[18,19] The d−π* character in the emitting state of such a complex dominates the kinetics of the deactivation processes by effective spin−orbit coupling with singlet excited states. The evaluated d−π* characters in T_1 of Pt(dpb)Cl and Pt(dpt)Cl are considered to be consistent with the reported emission lifetimes (7−8 μs[9]) as well as the emission energy shifts from the corresponding free ligands (2200−2600 cm^{-1}).

It should be mentioned that the d−π* character in T_1 does not lead to large $\Delta\mu_z$, the difference in dipole moment between the ground and excited state, for the objective complexes despite its charge-transfer nature. The d−π* character combined with the small $\Delta\mu_z$ in T_1 is clearly shown in Figure 5, which depicts the dominant charge flow from Pt, Cl, and phenyl ring to both pyridine rings in the tridentate ligand that cancel each other in the *y*-axis, thus exhibiting little change along the dipole moment in the *z*-axis. On the other hand, S_1 of Pt(dpb)Cl was calculated to have a considerably larger $\Delta\mu_z$ (−9.07 D) than T_1, in contrast to the small differences in the d−π* character between T_1 (25%) and S_1 (32%). The charge flow in S_1 is almost "straightforward"

TABLE 5: Orbital Populations on Pt for the Ground and Excited States from Mulliken Population Analysis[a]

	orbital population (difference from S_0)				
state	s	p_π[b]	p_σ[b]	d_π[b]	d_σ[b]
Pt(dpb)Cl					
S_0	2.71	2.09	4.12	3.78	4.74
T_1	2.71 (0.00)	2.15 (0.06)	4.12 (0.00)	3.53 (−0.25)	4.74 (0.00)
S_1	2.71 (0.00)	2.09 (0.00)	4.12 (0.00)	3.46 (−0.32)	4.74 (0.00)
Pt(dpt)Cl					
S_0	2.71	2.09	4.12	3.83	4.69
T_1	2.71 (0.00)	2.14 (0.05)	4.12 (0.00)	3.58 (−0.25)	4.69 (0.00)
S_1	2.71 (0.00)	2.09 (0.00)	4.12 (0.00)	3.51 (−0.32)	4.70 (0.00)

[a] Orbital populations are given in unit electron charge. Inner core electrons (1s through 4f) are not included because they are replaced by the effective core potential (ECP). [b] σ and π represent symmetrical and antisymmetrical orbitals about the molecular plane, respectively.

from the Pt and Cl to the phenyl ring that causes a large dipole moment change parallel to the *z*-axis.

4.3. Comparison of Phosphorescence Spectra of the Complexes and Free Ligands: Methyl Substitution Effects and Spectral Features. The methyl substitution causes a substantial decrease in phosphorescence 0−0 energy from Pt(dpb)Cl to Pt(dpt)Cl (540 cm^{-1}), while the difference between the free ligands (dpbH and dptH) is small (160 cm^{-1}), as explained in section 3.2. These calculations reproduced the differences in the T_1 excitation energies (362 cm^{-1} between the complexes and 127 cm^{-1} between the free ligands). The difference in the methyl substitution effect between the complexes and the free ligands can be assigned to the different orbital nature of T_1 in respective species. Although T_1 of Pt(dpb)Cl and dpbH have identical symmetry (A_1), they differ in dominant orbital excitations [$b_1 \rightarrow b_1^*$ for Pt(dpb)Cl; $a_2 \rightarrow a_2^*$ for dpbH]. The π orbitals of a_2 symmetry in dpbH [as well as Pt(dpb)Cl] have no component at the atoms on the symmetry axis, including C(4), as shown in the MO plots (Figure 4). The methyl substitution at C(4) is expected to have a minimal effect on the orbitals of a_2 symmetry as well as the $a_2 \rightarrow a_2^*$ excitations. On the other hand, the b_1 orbital (HOMO) of Pt(dpb)Cl spreads over C(4); hence, it resulted in a substantial difference in T_1 excitation energies between Pt(dpb)Cl and Pt(dpt)Cl.

The difference in the dominant orbital excitations between the complexes and the free ligands stated above gives valuable information about the phosphorescence spectra of these species. The phosphorescence spectra of the free ligands (Figure 3) show increased vibrational progressions compared to those of the complexes. These spectral features can be explained from the plots of the changes of electron density (Figure 5) that show the difference in T_1 character between Pt(dpb)Cl and dpbH. The changes of the electron density are found on the *atoms* for Pt(dpb)Cl, whereas those for dpbH, which show some resemblance to those for T_3 of Pt(dpb)Cl, are found mainly on the *bonds* in the phenyl ring and between the phenyl and pyridine rings. These electron-density changes on the bonds, especially in the phenyl ring, are expected to induce significant geometry changes for the free ligands between T_1 and S_0. These geometry changes appear as strong vibrational progressions in the phosphorescence spectra with frequencies of aromatic ring stretching about 1300 cm^{-1}. The geometry changes expected by the electron density calculations were confirmed by T_1 geometry optimizations for Pt(dpb)Cl and dpbH at the restricted open-shell B3LYP level. Geometries were optimized in C_{2v} symmetry and then compared to their S_0 structures. Particular attention was paid to selection of the initial-guess orbitals for the SCF calculations in T_1 geometry optimizations to obtain coherent results with the TDDFT calculations about nature of the singly occupied orbitals. Table 6 summarizes the changes in bond length between S_0 and T_1. For dpbH, the length of the C(2)−C(3) bond shows a notable increase (0.085 Å) by excitation to T_1 that is consistent with the electron density plot (Figure 5), while changes in bond length for Pt(dpb)Cl are rather small compared to those for dpbH, and mainly observed for the bonds between Pt and its neighboring atoms [Cl and C(1)].

Additional TDDFT calculations were carried out for both Pt(dpb)Cl and dpbH at the T_1 optimized geometry to obtain the relaxation energy in T_1 (the difference between the T_1 energies at the S_0 and T_1 optimized geometries) and the adiabatic T_1 excitation energy (the vertical T_1 excitation energy at the S_0 optimized geometry minus the relaxation energy in T_1). The obtained T_1 relaxation energy for Pt(dpb)Cl (631 cm^{-1}) is notably smaller than that of dpbH (2070 cm^{-1}); this result is consistent with the above discussion on the phosphorescence profiles of Pt(dpb)Cl and dpbH. The adiabatic T_1 excitation energies are figured out to be 19 790 cm^{-1} for Pt(dpb)Cl and 21 274 cm^{-1} for dpbH; these values are in good agreement with the experimental 0−0 excitation energies in S_0-T_1 transitions.

TABLE 6: Calculated Bond Lengths and Differences between S_0 and T_1 of Pt(dpb)Cl and DpbH[a]

	Pt(dpb)Cl[b]			dpbH[b]		
bond[c]	S_0	T_1	difference	S_0	T_1	difference
Pt−Cl	2.471	2.444	−0.027			
Pt−C(1)	1.926	1.899	−0.027			
Pt−N	2.065	2.063	−0.002			
C(1)−C(2)	1.403	1.434	0.031	1.402	1.397	−0.005
C(2)−C(3)	1.402	1.390	−0.012	1.405	1.490	0.085
C(3)−C(4)	1.401	1.412	0.011	1.393	1.386	−0.007
C(2)−C(5)	1.469	1.451	−0.018	1.492	1.442	−0.050
C(5)−C(6)	1.397	1.397	0.000	1.406	1.424	0.018
C(6)−C(7)	1.392	1.390	−0.002	1.392	1.388	−0.004
C(7)−C(8)	1.395	1.408	0.013	1.393	1.395	0.002
C(8)−C(9)	1.391	1.385	−0.006	1.396	1.408	0.012
C(9)−N	1.343	1.351	0.008	1.333	1.321	−0.012
C(5)−N	1.379	1.398	0.019	1.347	1.369	0.022

[a] Bond lengths are given in angstroms. [b] Geometries are optimized within the symmetry constraint of C_{2v}. [c] See Figure 1 for numbering of the carbon atoms.

5. Conclusion

The lowest triplet and singlet excited states (T_1 and S_1) of the objective complexes Pt(dpb)Cl and Pt(dpt)Cl have been assigned to $^3A_1(b_1 \rightarrow b_1^*)$ and $^1B_2(b_1 \rightarrow a_2^*)$, respectively, from the TDDFT calculations with the assistance of the observed spectroscopic properties. The calculated excitation energies for T_1 and S_1 of the complexes show good agreement with their respective observed values within 600 cm^{-1}. These states are predicted to have mixed characters of $d-\pi^*$ and $\pi-\pi^*$ excitations. On the basis of the single excitation nature of the TDDFT approach, the $d-\pi^*$ character in excited states is evaluated from the decrease in the d-electron densities on Pt by excitation; values of 25% for T_1 and 32% for S_1 have been obtained for both complexes. The emitting states of the free ligands (dpbH and dptH) are predicted to be different in orbital nature from those of the complexes; this difference in orbital nature explains the observed difference in methyl-substitution effect as well as different emission profiles between the complexes and the free ligands. Other spectroscopic features of the complexes, such as the negative solvatochromic shift and small Stokes shift, are also successfully explained from the calculation results based on the above assignment.

The above results have proved that the TDDFT approach is rational for analysis of the excited-state properties of the objective complexes. The presented procedure to evaluate the $d-\pi^*$ character may be a useful tool to design highly phosphorescent complexes. We consider that it is very important to conduct further studies to evaluate $d-\pi^*$ character in the excited states of a variety of phosphorescent complexes and then to investigate the relationship between the $d-\pi^*$ character and phosphorescence properties of these complexes in order to get an in-depth understanding of the photophysics of the complexes.

Acknowledgment. We thank Dr. N. F. Cooray for helpful suggestions and discussions.

References and Notes

(1) Baldo, M. A.; O'Brien, D. F.; You, Y.; Shoustikov, A.; Sibley, S.; Thompson, M. E.; Forrest, S. R. *Nature (London)* **1998**, *395*, 151.

(2) Baldo, M. A.; Lamansky, S.; Burrows, P. E.; Thompson, M. E.; Forrest, S. R. *Appl. Phys. Lett.* **1999**, *75*, 4.
(3) Lamansky, S.; Djurovich, P.; Murphy, D.; Abdel-Razzaq, F.; Kwong, R.; Tsyba, I.; Bortz, M.; Mui, B.; Bau, R.; Thompson, M. E. *Inorg. Chem.* **2001**, *40*, 1704.
(4) Lamansky, S.; Djurovich, P.; Murphy, D.; Abdel-Razzaq, F.; Lee, H.-E.; Adachi, C.; Burrows, P. E.; Forrest, S. R.; Thompson, M. E. *J. Am. Chem. Soc.* **2001**, *123*, 4304.
(5) Carlson, B.; Phelan, G. D.; Kaminsky, W.; Dalton, L.; Jiang, X.; Liu, S.; Jen, A. K.-Y. *J. Am. Chem. Soc.* **2002**, *124*, 14162.
(6) Tamayo, A. B.; Alleyne, B. D.; Djurovich, P. I.; Lamansky, S.; Tsyba, I.; Ho, N. N.; Bau, R.; Thompson, M. E. *J. Am. Chem. Soc.* **2003**, *125*, 7377.
(7) Tsuboyama, A.; Iwawaki, H.; Furugori, M.; Mukaide, T.; Kamatani, J.; Igawa, S.; Moriyama, T.; Miura, S.; Takiguchi, T.; Okada, S.; Hoshino, M.; Ueno, K. *J. Am. Chem. Soc.* **2003**, *125*, 12971.
(8) Cárdenas, D. J.; Echavarren, A. M.; Ramírez de Arellano, M. C. *Organometallics* **1999**, *18*, 3337.
(9) Williams, J. A. G.; Beeby, A.; Davies, E. S.; Weinstein, J. A.; Wilson, C. *Inorg. Chem.* **2003**, *42*, 8609.
(10) Sotoyama, W.; Satoh, T.; Sawatari, N.; Inoue, H. *Appl. Phys. Lett.* **2005**, *86*, 153505.
(11) Hay, P. J. *J. Phys. Chem. A* **2002**, *106*, 1634.
(12) Finkenzeller, W. J.; Yersin, H. *Chem. Phys. Lett.* **2003**, *377*, 299.
(13) King, K. A.; Spellane, P. J.; Watts, R. J. *J. Am. Chem. Soc.* **1985**, *107*, 1431.
(14) Watts, R. J.; Crosby, G. A.; Sansregret, J. L. *Inorg. Chem.* **1972**, *11*, 1474.
(15) Crosby, G. A. *Acc. Chem. Res.* **1975**, *8*, 231.
(16) Azumi, T.; Miki, H. *Top. Curr. Chem.* **1997**, *191*, 1.
(17) Yersin, H.; Humbs, W.; Strasser, J. *Top. Curr. Chem.* **1997**, *191*, 153.
(18) Yersin, H.; Donges, D. *Top. Curr. Chem.* **2001**, *214*, 81.
(19) Yersin, H. *Top. Curr. Chem.* **2004**, *241*, 1.
(20) Yersin, H.; Donges. D.; Humbs, W.; Strasser, J.; Sitters, R.; Glasbeek, M. *Inorg. Chem.* **2002**, *41*, 4915.
(21) Giesbergen, C.; Glasbeek, M. *J. Phys. Chem.* **1993**, *97*, 9942.
(22) Miki, H.; Shimada, M.; Azumi, T.; Brozik, J. A.; Crosby, G. A. *J. Phys. Chem.* **1993**, *97*, 11175.
(23) Connick, W. B.; Miskowski, V. M.; Houlding, V. H.; Gray, H. B. *Inorg. Chem.* **2000**, *39*, 2585.
(24) Jamorski, C.; Casida, M. E.; Salahub, D. R. *J. Chem. Phys.* **1996**, *104*, 5134.
(25) Petersilka, M.; Gossmann, U. J.; Gross, E. K. U. *Phys. Rev. Lett.* **1996**, *76*, 1212.
(26) Stratmann, R. E.; Scuseria, G. E.; Frisch, M. J. *J. Chem. Phys.* **1998**, *109*, 8218.
(27) Frisch, M. J.; Trucks, G. W.; Schlegel, H. B.; Scuseria, G. E.; Robb, M. A.; Cheeseman, J. R.; Zakrzewski, V. G.; Montgomery, J. A., Jr.; Stratmann, R. E.; Burant, J. C.; Dapprich, S.; Millam, J. M.; Daniels, A. D.; Kudin, K. N.; Strain, M. C.; Farkas, O.; Tomasi, J.; Barone, V.; Cossi, M.; Cammi, R.; Mennucci, B.; Pomelli, C.; Adamo, C.; Clifford, S.; Ochterski, J.; Petersson, G. A.; Ayala, P. Y.; Cui, Q.; Morokuma, K.; Malick, D. K.; Rabuck, A. D.; Raghavachari, K.; Foresman, J. B.; Cioslowski, J.; Ortiz, J. V.; Baboul, A. G.; Stefanov, B. B.; Liu, G.; Liashenko, A.; Piskorz, P.; Komaromi, I.; Gomperts, R.; Martin, R. L.; Fox, D. J.; Keith, T.; Al-Laham, M. A.; Peng, C. Y.; Nanayakkara, A.; Gonzalez, C.; Challacombe, M.; Gill, P. M. W.; Johnson, B.; Chen, W.; Wong, M. W.; Andres, J. L.; Gonzalez, C.; Head-Gordon, M.; Replogle, E. S.; Pople, J. A. *Gaussian 98*, Revision A.7; Gaussian, Inc.: Pittsburgh, PA, 1998.
(28) van Gisbergen, S. J. A.; Groeneveld, J. A.; Rosa, A.; Snijders, J. G.; Baerends, E. J. *J. Phys. Chem. A* **1999**, *103*, 6835.
(29) Campbell, I. H.; Smith, D. L.; Tretiak, S.; Martin, R. L.; Neef, C. J.; Ferraris, J. P. *Phys. Rev. B* **2002**, *65*, 085210.
(30) Xie, Z.-Z.; Fang, W.-H. *J. Mol. Struct. THEOCHEM* **2005**, *717*, 179.
(31) Yang, L.; Ren, A.-M.; Feng, J.-K.; Liu, X.-J.; Ma, Y.-G.; Zhang, M.; Liu, X.-D.; Shen, J.-C.; Zhang, H.-X. *J. Phys. Chem. A* **2004**, *108*, 6797.
(32) Gunaratne, T. C.; Gusev, A. V.; Peng, X.; Rosa, A.; Ricciardi, G.; Baerends, E. J.; Rizzoli, C.; Kenney, M. E.; Rodgers, M. A. *J. Phys. Chem. A* **2005**, *109*, 2078.
(33) Batista, E. R.; Martin, R. L. *J. Phys. Chem. A* **2005**, *109*, 3128.
(34) Polson, M.; Ravaglia, M.; Fracasso, S.; Garavelli, M.; Scandola, F. *Inorg. Chem.* **2005**, *44*, 1282.
(35) Hay, P. J.; Wadt, W. R. *J. Chem. Phys.* **1985**, *82*, 299.
(36) Hayano, T. *MOPAC2002 V1*, *xmo* version 4.0, Fujitsu Ltd, Tokyo, Japan, 2001.
(37) Lee, C.; Yang, W.; Parr, R. G. *Phys. Rev. B* **1988**, *37*, 785.
(38) Becke, A. D. *J. Chem. Phys.* **1993**, *98*, 5648.
(39) Marcus, R. A. *J. Chem. Phys.* **1965**, *43*, 1261.
(40) Wilde, A. P.; Watts, R. J. *J. Phys. Chem.* **1991**, *95*, 622.
(41) Maestri, M.; Sandrini, D.; Balzani, V.; von Zelewsky, A.; Deuschel-Cornioley, C.; Jolliet, P. *Helv. Chim. Acta* **1988**, *71*, 1053.
(42) Wiedenhofer, H.; Schützenmeier, S.; von Zelewsky, A.; Yersin, H. *J. Phys. Chem.* **1995**, *99*, 13385.
(43) Tozer, D. J. *J. Chem. Phys.* **2003**, *119*, 12697.
(44) Dreuw, A.; Weisman, J. L.; Head-Gordon, M. *J. Chem. Phys.* **2003**, *119*, 2943.
(45) Dreuw, A.; Head-Gordon, M. *J. Am. Chem. Soc.* **2004**, *126*, 4007.
(46) Turki, M.; Daniel, C.; Záliš, S.; Vlček, A., Jr.; van Slageren, J.; Stufkens, D. J. *J. Am. Chem. Soc.* **2001**, *123*, 11431.
(47) Pierloot, K.; Ceulemans, A.; Merchán, M.; Serrano-Andrés, L. *J. Phys. Chem. A* **2000**, *104*, 4374.
(48) Wiberg, K. B.; Haded, C. M.; Foresman, J. B.; Chupka, W. A. *J. Phys. Chem.* **1992**, *96*, 10756.
(49) Hirata, S.; Head-Gordon, M. *Chem. Phys. Lett.* **1999**, *302*, 375.